HIGH PRECISION PHOTON FLUX DETERMINATION FOR PHOTON TAGGING EXPERIMENTS

A. Teymurazyan[a], A. Ahmidouch[b], P. Ambrozewicz[b], A. Asratyan[c], K. Baker[d], L. Benton[b], V. Burkert[f], E. Clinton[g], P. Cole[h], P. Collins[i], D. Dale[h], S. Danagoulian[b], G. Davidenko[c], R. Demirchyan[b], A. Deur[f], A. Dolgolenko[c], G. Dzyubenko[c], R. Ent[f], A. Evdokimov[c], J. Feng[j,k], M. Gabrielyan[a], L. Gan[j], A. Gasparian[b], A. Glamazdin[n], V. Goryachev[c], K. Hardy[b], J. He[o], M. Ito[f], L. Jiang[j,k], D. Kashy[f], M. Khandaker[h], A. Kolarkar[a], M. Konchatnyi[n], A. Korchin[n], W. Korsch[a], O. Kosinov[h], S. Kowalski[e], M. Kubantsev[c,q], V. Kubarovsky[f], I. Larin[b,c], D. Lawrence[f,g], X. Li[j], P. Martel[g], V. Matveev[c], D. McNulty[h], B. Mecking[f], B. Milbrath[r], R. Minehart[s], R. Miskimen[g], V. Mochalov[t], I. Nakagawa[a,u], S. Overby[b], E. Pasyuk[f,i], M. Payen[b], R. Pedroni[b], Y. Prok[e], B. Ritchie[i], C. Salgado[p], A. Shahinyan[l], A. Sitnikov[c], D. Sober[w], S. Stepanyan[f], W. Stevens[s], J. Underwood[b], A. Vasiliev[t], V. Vishnyakov[c], M. Wood[g], S. Zhou[j]

[a]*University of Kentucky, Lexington, KY 40506, USA*
[b]*North Carolina A&T State University, Greensboro, NC 27411, USA*
[c]*Alikhanov Institute for Theoretical and Experimental Physics, Moscow, Russia*
[d]*Hampton University, Hampton, VA 23606, USA*
[e]*Massachusetts Institute of Technology, Cambridge, MA 02139. USA*
[f]*Thomas Jefferson National Accelerator Facility, Newport News, VA 23606, USA*
[g]*University of Massachusetts, Amherst, MA 01003, USA*
[h]*Idaho State University, Pocatello, ID 83209, USA*
[i]*Arizona State University, Tempe, AZ 85287, USA*
[j]*University of North Carolina, Wilmington, Wilmington, NC 28403, USA*
[k]*Chinese Institute of Atomic Energy, Beijing, China*
[l]*Yerevan Physics Institute, Yerevan, Armenia*
[m]*Joint Institute for Nuclear Research, Dubna, 141980, Russia*
[n]*Kharkov Institute of Physics and Technology, Kharkov, Ukraine*
[o]*Institute of High Energy Physics, Chinese Academy of Sciences, Beijing, China*
[p]*Norfolk State University, Norfolk, VA 23504, USA*
[q]*Northwestern University, Evanston/Chicago, IL 60208, USA*
[r]*Pacific Northwest National Laboratory, Richland, WA 99352, USA*
[s]*University of Virginia, Charlottesville, VA 22094, USA*
[t]*Institute for High Energy Physics, Protvino, Russia*
[u]*RIKEN Nishina Center for Accelerator-Based Science, 2-1 Hirasaw, Wako, Saitama 351-0198, Japan*
[v]*University of Sao Paulo, Sao Paulo, Brazil*
[w]*The Catholic University of America, Washington, DC 20064, USA*

Abstract

The Jefferson Laboratory *PrimEx* Collaboration has developed and implemented a method to control the tagged photon flux in photoproduction experiments at the 1% level over the photon energy range from 4.9 to 5.5 GeV. This method has been successfully implemented in a high precision measurement of the neutral pion lifetime. Here, we outline the experimental equipment and the analysis techniques used to accomplish this. These include the use of a total absorption counter for absolute flux calibration, a pair spectrometer for online relative flux monitoring, and a new method for postbremsstrahlung electron counting.

Keywords: photon tagging, pair spectrometer, photonuclear reactions

1. Introduction

The photon tagging technique has been used routinely in various forms [1–9] to provide quasimonochromatic photons for absolute photonuclear cross section measurements. The analysis of such experiments in the context of bremsstrahlung photon tagging was summarized by Owens in 1990 [10]. Since then, a number of developments have made possible significant improvements in the implementation of this technique. Here, we describe the steps taken by the *PrimEx* Collaboration in Hall B of Jefferson Laboratory to limit the systematic uncertainty in the absolute photon flux to the 1% level. They include an absolute flux calibration at low intensity with a total absorption counter, online relative flux monitoring with a pair spectrometer, and the use of multi-hit time to digital converters for post bremsstrahlung electron counting during production data runs. While this discussion focuses on the analysis techniques utilized by the *PrimEx* Collaboration which involves a bremsstrahlung based photon tagging system to measure the neutral pion lifetime, the methods described herein readily apply to other types of photon tagging system.

2. The *PrimEx* Experimental setup

The goal of the *PrimEx* experiment is to perform a precise measurement of the cross section for photoproduction of neutral pions in the Coulomb field of a nucleus (the Primakoff effect)[13]. The primary equipment in the experiment includes (see Fig. 1): (1) the Hall B photon tagger; (2) solid π^o production targets (C, Si, and Pb) of thickness 5-10% of a radiation length (r.l.); (3) a sweeping magnet/pair spectrometer located after the production targets; (4) a 1.16m $\times$ 1.16m highly segmented lead glass photon detector for π^o decay photons, with a high resolution $PbWO_4$ insertion in the central region near the beam and a plastic scintillator charged particle veto [12].

3. Photon tagging in Hall B of Jefferson Lab

Jefferson Lab (JLab) Hall B photon experiments utilize the well known bremsstrahlung photon tagging technique to measure the energy and time information of incident photons in real photon induced reactions [9]. The electron beam of initial energy E_0 (in the case of *PrimEx* $E_0 = 5.76$ GeV) is incident upon a thin ($3 \times 10^{-4}, 10^{-4}$ or 10^{-5} r.l.) gold bremsstrahlung radiator foil. The electron loses energy in the electromagnetic field of the nucleus and in the process emits a bremsstrahlung photon. The number of photons with energies in the interval k — $k + dk$ is approximately proportional to the Z^2 of the radiator and, over most of the photon energy range, is approximately inversely proportional to the energy k of the photons [14]. Due to the relatively small mass of the electron the recoil energy transferred to the nucleus is negligible, and the bremsstrahlung photon energy can be written as:

$$E_\gamma = E_0 - E_e \tag{1}$$

where E_γ is the energy of the bremsstrahlung photon and E_e is the energy of the post-bremsstrahlung electron. In the case of Hall B of Jefferson Laboratory, the energy E_0 of the electrons incident on the radiator is determined at the

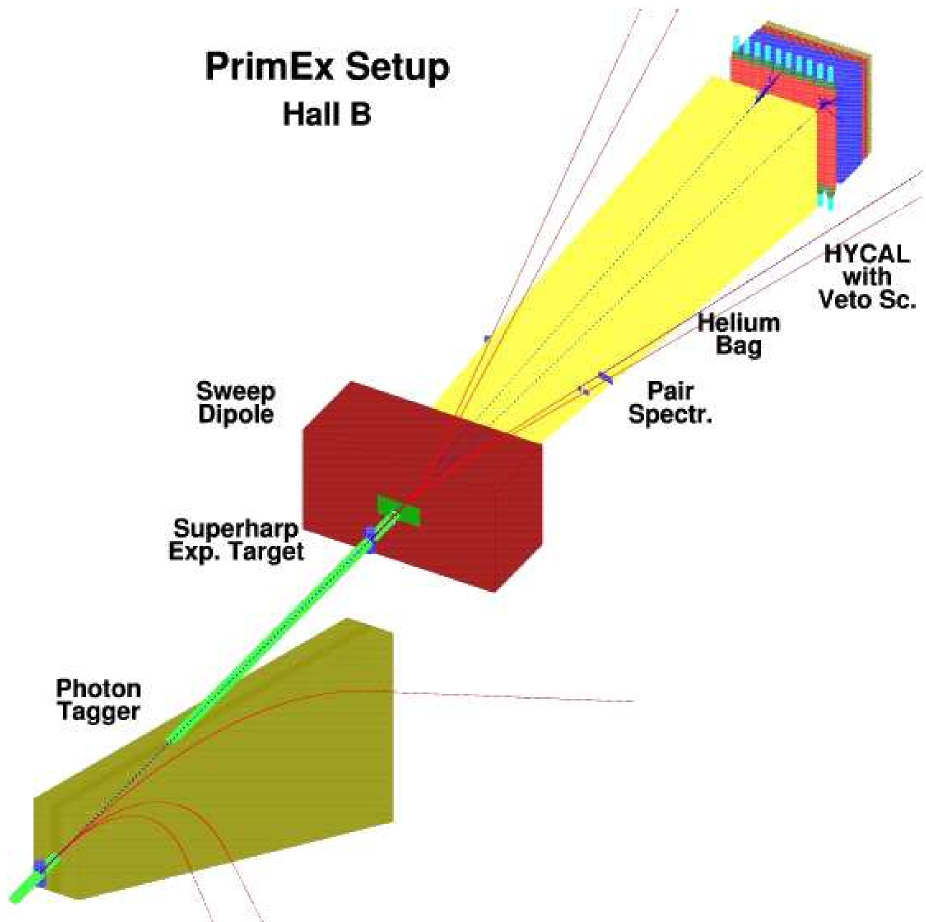

Figure 1: Layout of the *PrimEx* experimental setup.

10^{-4} level by their trajectories through the arc magnets of the accelerator[15]. Thus, one can determine the energy of the photon by measuring the energy of the post-bremsstrahlung electron.

The main components of the Jefferson Lab Hall B photon tagger are a thin bremsstrahlung radiator, a dipole magnet capable of a full field of 1.75 T and two rows of plastic scintillator hodoscopes. The photons produced in the radiator continue through the tagger, toward the physics target 7.1 meters downstream in the experimental hall. For the *PrimEx* experiment, a 12.7 mm diameter clean-up collimator placed 6.6 meters from the radiator in conjunction with a

0.73 T permanent magnet are centered on the photon beam line in order to limit the transverse extent of the photon beam. Post bremsstrahlung electrons are separated from the photons by the tagger dipole magnet. The field setting of the magnet is adjusted according to the incident beam energy to allow full energy electrons which do not interact in the radiator to be transported into a shielded beam dump below the floor of the experimental hall. The energy-degraded electrons are detected in E-counters (for energy determination) and T- counters (for timing) that lie along a flat focal plane downstream from the straight edge of the magnet as described in reference [9].

The focal plane of the tagger is divided into two groups of T-counters. The first group of 19 counters covers the photon energy range from 77% to 95% of the incident electron energy, and the group of 42 remaining wider counters covers the range from 20% to 77%. The size of individual T-counters compensates for the $1/k$ behavior of the bremsstrahlung cross-section. The width of each T-counter is chosen in such a fashion that it enables approximately the same counting rate for each detector within the same group. When all 61 T-counters are used, the total tagging rate can be as high as 50 MHz for the whole focal plane. The high energy photon counters T1-T19 are proportionally smaller, and allow a tagging rate of up to 50 MHz in this region alone [9]. The *PrimEx* experiment used only the counters T1 (corresponding to $E_\gamma = 5.5$ GeV) through T11 ($E_\gamma = 4.9$ GeV).

The use of the Jefferson Lab Hall B photon tagging facility gives the *PrimEx* experiment several advantages over the previous experiments that were based on the Primakoff effect [16–20]. The angular dependence of the π^0 photoproduction cross section being measured is strongly dependent on the incident photon energy. The precise determination of the tagged photon flux on the experimental target is also enabled by the tagger. Thus a more accurate knowledge and control of the photon beam energy and the luminosity enables a greater control over systematic errors.

In order to determine the energy of the π^0, each event is recorded in coincidence with a signal from the tagger. The experimental cross section for neutral pion photoproduction is determined by the following expression:

$$\frac{d\sigma}{d\Omega} = \frac{dY_{\pi^0}^{tagged}}{N_{\gamma}^{tagged} \cdot \epsilon \cdot t \cdot d\Omega} \tag{2}$$

where $d\Omega$ is the element of solid angle of the pion detector, $dY_{\pi^0}^{tagged}$ is the yield of tagged π^0's within solid angle $d\Omega$, t is the target thickness, ϵ is a factor accounting for geometrical acceptance and energy dependent detection efficiency, and N_{γ}^{tagged} is the number of tagged photons on the target.

As can be seen from Equation 2, the normalization of the cross section directly depends on knowing the tagged photon flux on the target. The number of tagged photons is not equal to the number of hits recorded by the tagging counters because of a number of effects:

(1) events in which a bremsstrahlung photon is produced and then absorbed before reaching the target.

(2) processes, such as Møller scattering in the bremsstrahlung radiator, through which the main electron beam generates counts in the tagging counters without an accompanying photon.

(3) extra hits registered in the tagging counters due to (beam off) room background in the experimental hall.

To minimize the absorption of photons before they reach the target, the bremsstrahlung beam travels in vacuum. The Møller scattering events are thought to affect the tagging ratio at the level of a few percent[9]. The impact of the room background on the tagging rates of runs with various electron beam intensities is continuously monitored.

The combination of these effects can be measured in a calibration run by removing the physics target and placing a large acceptance lead-glass Total Absorption Counter (TAC) directly in the photon beam. Assuming that the total absorption counter is 100% efficient in detecting photons in the energy range relevant for the experiment (a GEANT simulation gave 99.97% efficiency for

4.6 GeV photons with a 1.1 GeV threshold), the ratio of Tagger-TAC coincidences to the number of tagger hits, the so called absolute tagging ratio, is then recorded:

$$R^i_{absolute} = \frac{N^{TAC}_{\gamma \cdot e^i}}{N^i_e} \tag{3}$$

where $N^{TAC}_{\gamma \cdot e^i}$ is the number of photons registered by the TAC in coincidence with a particular tagging counter and N^i_e is the number of counts in the same tagging counter. In these normalization measurements, the trigger is set to the OR of the tagging counters and N^i_e is determined by the number of events in the self timing peak in its TDC spectrum.

Knowing this ratio, one can determine the tagged photon flux in the data taking run by counting the number of post bremsstrahlung electrons in the tagging counters:

$$N^{tagged}_{\gamma}|_{experiment} = N_e|_{experiment} \times R_{absolute} \tag{4}$$

The use of the total absorption counter to calibrate the number of tagged photons per electron in the tagger provides an absolute normalization of the tagged photon flux incident on the π^0 production target. However, these measurements can be performed only at intervals interspersed throughout the data taking. Also in a calibration run, the rate of the total absorption counter is limited, and therefore, the tagging ratio can only be measured at a rate which is reduced by a factor of about one thousand as compared to the data taking run. As such, any rate and time dependence in the tagging ratio must be carefully considered. A pair production luminosity monitor was constructed which is able to measure the relative tagged photon flux over a range of all relevant intensities, and operate continuously throughout the data taking runs. The pair spectrometer (see Fig. 2) uses the physics target as a converter to measure the ratio of the number of $\gamma + A \rightarrow A + e^+ + e^-$ reactions in coincidence with a tagging signal to the number of hits in the tagging counters.

This enables one to measure a relative tagging ratio:

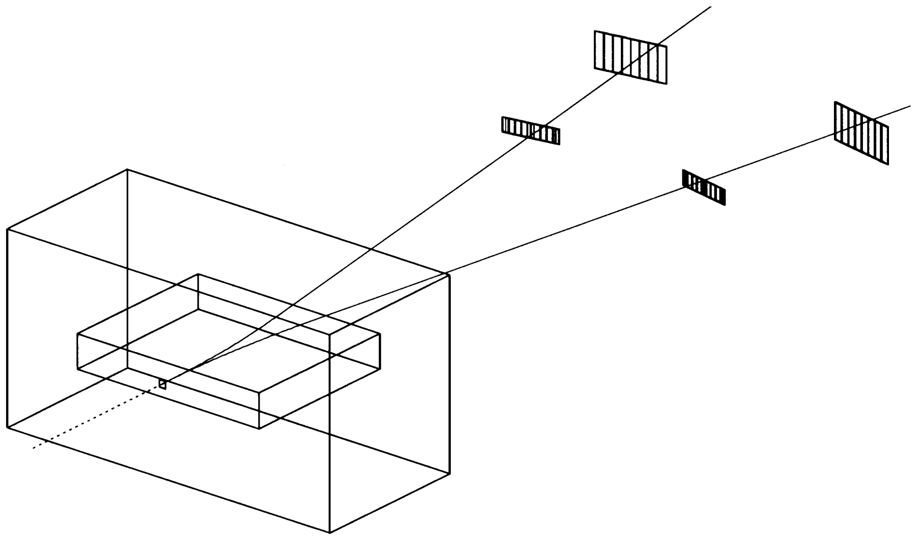

Figure 2: A schematic layout of the pair spectrometer. Each arm consists of eight contiguous plastic scintillator hodoscopes in each row.

$$R^i_{relative} = \frac{N^{PS}_{e^+e^-\cdot e^i}}{N^i_e} \tag{5}$$

where in analogy with Eq. 3, $N^{PS}_{e^+e^-\cdot e^i}$ is the number of pair spectrometer counts in coincidence with a given tagging counter, and N^i_e is the number of counts in a tagging counter. While this is a relative number, its absolute normalization can be determined with the TAC.

The advantages of the pair spectrometer are that it can operate over the entire range of intensities of both the flux calibration with the TAC and the production data taking runs, and has a smooth, relatively flat acceptance in E_γ covering the entire tagging range. The segmentation of the pair spectrometer detectors is driven by the fact that the pair production and Primakoff target are the same, and therefore the pair spectrometer detectors must accommodate the rates from a $5-10\%$ radiation length target. Under the *PrimEx* run conditions, singles rates on a single telescope were about 140 kHz, and totaled 90 kHz of PS-Tagger coincidences over the range of tagging energies. The measured efficiency of the pair spectrometer for detecting tagged photons was about 0.5%. The upstream plastic scintillators were instrumented with Hamamatsu R6427 photomultiplier tubes, while the downstream detectors were coupled to Hamamatsu R580-17 photomultiplier tubes. Each of the scintillator detector signals was discriminated with a CAEN N413A non-updating discriminator and timing information was recorded in a TDC (LeCroy LRS1877). In the analysis, the electron-positron coincidences were made in software via matching of the timing signals.

To reduce the data acquisition rates, the primary trigger was provided by the tagged photons in coincidence with the electromagnetic calorimeter. In the yield, one counts only π^0 events which are in prompt coincidence with the tagger. The N_γ^{tagged} in the denominator of Equation 2 has to be counted consistent with the way $Y_{\pi^0}^{tagged}$ is determined. This means that if events are discarded from the yield calculation, they should not be considered when calculating the photon flux either, and vice versa. Further, triggering on the calorimeter signal plus tagger in the production runs as opposed to just the tagger has implications in the determination of the number of post bremsstrahlung electrons in the tagger. This will be discussed below.

4. Determination of the absolute tagging ratios

In the calibration runs designed to measure the absolute tagging ratios, the experimental target was retracted and the Total Absorption Counter (TAC) was placed in the path of the photon beam 17 meters downstream of the radiator. This detector consists of a single $20\times20\times40 cm^3$ lead glass block (SF5, L = 17 r.l.). It has a single 5" attached Hamamatsu photomultiplier tube (R1250, 2.5 nanosecond rise time) and is instrumented with a LeCroy 4413 16 channel programmable discriminator, a TDC, and an ADC. With a 100 pA electron beam current and a 2×10^{-5} r.l. bremsstrahlung radiator, it triggered at about 100 kHz with a 35 mV threshold, which corresponds to 0.66 GeV, the energy threshold used during the *PrimEx* run. To avoid radiation damage to the TAC, the electron beam intensity was typically $\sim 70-80$ pA. Such a low intensity of the electron beam enables the use of the Tagger Master-OR (MOR) signal as the data acquisition trigger. The MOR signal is formed by OR-ing the timing information from all or any of the 11 T-counters. The MOR trigger enables one to determine the number of electrons that hit a given tagging counter from the number of counts in its self timing TDC peak.

Absolute tagging ratios are then defined for each of the T-counters as in equation 3. A number of measurements were performed to investigate the robustness of this procedure and are outlined in the following sections.

5. Systematic effects relating to photon flux determination

5.1. Tagger backgrounds

Data taking runs were typically of one to two hours in duration. At the beginning of each run, photon tagger data was taken for ten seconds with the beam off. The Master-OR rate (the OR of the 11 T counters used in this experiment) with the beam off was typically a few hundred Hz. For the absolute calibration measurements with 70-80 pA beam current, the MOR rate was typically a factor of one thousand higher than this. While this room background is quite small, these rates were measured without the geometric matching of the E and T counters. Such a matching gives considerable improvement on top of this already low background. In addition, an algorithm was implemented to ensure that data during and around beam trips were not analyzed.

5.2. TAC - Tagger coincidence and random background determination

The spectrum of tagger-TAC time differences exhibits a coincidence peak and a random background. Figure 3 shows a typical coincidence spectrum for the TAC-Tagger coincidence. Note that the signal to background ratio is better than 10000 : 1, and thus the determination of the number of prompt coincidences is quite insensitive to the accuracy of the background estimation procedure.

From Fig. 3 one can see that the background is not uniform on either side of the coincidence peak. In particular, the dip around ~ 5 to 40 ns to the right of

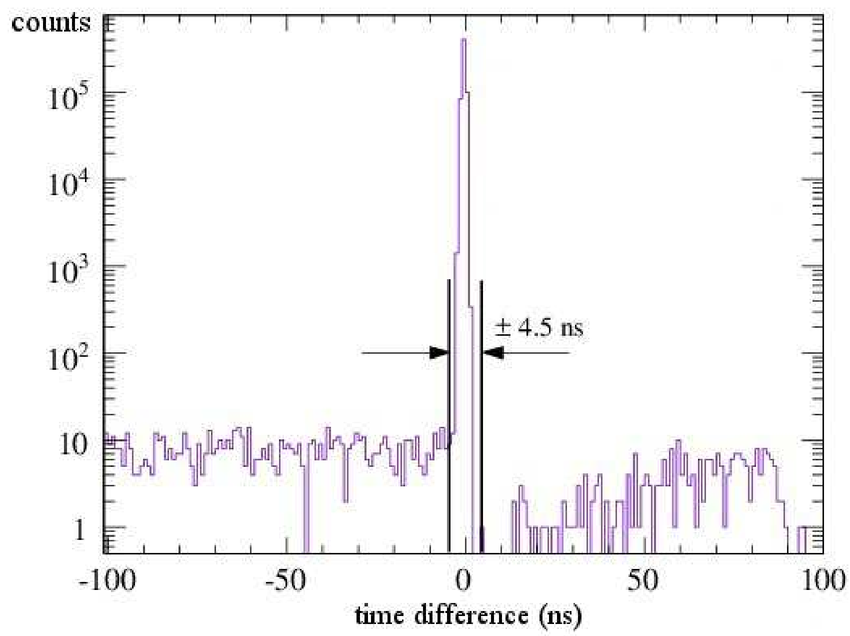

Figure 3: Distribution of time differences for events reconstructed for a single tagging counter and the TAC showing the ±4.5 ns timing window for coincidence events.

the coincidence peak is due to the TDC dead time. To determine the number of TAC-Tagger coincidences, a ±4.5 ns window was set up around the peak. Because of the nonuniformity of the background, a 4.5 μs window, from 7 to 4500 ns, was taken only on the left side of the coincidence peak to calculate the background level, which was taken to be flat and uniform with the introduction of negligible error.

5.3. Effects of incident electron beam intensity on absolute tagging ratios

Since the flux calibration and production data taking runs are performed under different beam conditions, it is important to demonstrate that the tagging ratios obtained at beam intensities of $\sim$ 80 pA are valid when applied to the data collected at the high beam intensities of about 80 to 130 nA. One means to investigate this involved normalization runs with various beam intensities

(40 − 120 pA).

No noticeable systematic dependence of tagging ratios on the incident beam intensity was detected when varying the beam intensity from 40 to 120 pA and the maximum deviation from the mean tagging ratio for each of the "T" counters was less than 0.4%. While this study involves only a limited range of intensities, a more complete answer to the question of intensity dependence of tagging ratios can be found by looking at relative tagging ratios where the beam intensity can be changed anywhere from < 80pA to 100 − 150 nA. This will be discussed later in this paper.

5.4. Long and short term reproducibility

To test our ability to perform a consistent measurement of the absolute tagging ratios, $R_{absolute}$, back-to-back normalization runs were performed with the 12.7 mm collimator removed at times 20 to 25 minutes apart. This study showed that four consecutive runs agree to within less than 0.3%, within the limits of the required precision and statistical errors.

To investigate longer term reproducibility, Fig. 4 (top) shows the results of absolute tagging ratios measured approximately four and a half hours and five days apart. Figure 4 (bottom) shows the percent deviation of the tagging ratio for each T-counter from the relevant average value. The statistical error for each point is on the order of 0.2%. As seen from the plots, all three measurements are in very good agreement with each other.

5.5. Effects of photon collimator misalignment

To study the sensitivity of the tagging ratios on the beam position with respect to the collimator, measurements for five different collimator positions were performed and are shown in Figure 5 (top). Figure 5 (bottom) shows the percent deviation of tagging ratios, measured at different displacements of the collimator transverse to the beam, from the value which was measured with the collimator in its nominal centered position (*i.e.,* at 7.02″). During the *PrimEx* run, typical measured beam position variations at the photon collimator were less than 0.5 mm. From Figure 5 (bottom) one can see that the shift in collimator position from 7.02″ to 7.15″ - a 3.3 mm displacement - lowers the absolute tagging ratios by about 0.34%, indicating a negligible contribution to the photon flux error budget due small drifts in beam position.

5.6. Effects of collimator diameter

The *PrimEx* experiment ran with very loose collimation of the bremsstrahlung photon beam to cut out the beam halo and increase the stability of the luminosity by keeping the photon beam very near to one spot on the target.

In Fig. 6 (top) the relative tagging ratios are plotted versus T-counter ID for data taken with two different collimators. For reference purposes a result with no collimation is also plotted. Note that for these measurements the statistical error on each point is on the order of 0.15%. As indicated in Fig. 6 (bottom), the 12.7 mm diameter collimator cuts out $\sim$ 1% of the photon beam and the 8.6 mm diameter collimator cuts out $\sim$ 4% of the photon beam.

6. Normalization of the production data runs

As indicated in Eq. 4, a key element in measuring the tagged photon flux is the counting of the post bremsstrahlung electrons in the tagger. For most tagged photon experiments at JLab including *PrimEx*, photons are produced at a rate far greater than is practical for direct counting by the data acquisition system. The exception to this is the TAC calibration runs where, as mentioned above, the rates are lower by a factor of one thousand.

The traditional technique to measure normalization involves hardware scalers that are used to count the number of hits in a particular tagging counter. Scalers have the advantage of being able to count virtually all the hits from a detector. Also, using scalers to measure the detector rates can automatically account for beam-trips, *i.e.* uncontrolled beam intensity drops or spikes, provided that the scalers count signals from a beam related source. However the triggering scheme used for the *PrimEx* experiment makes the hardware scaler method unattractive exactly due to the fact that scalers would count all the hits in the tagging counters.

The primary trigger for the *PrimEx* experiment was formed by a coincidence of signals from the electromagnetic calorimeter and the tagger. When the total energy deposited in the calorimeter exceeded a threshold of 2.4 GeV and there is a signal available from the tagger, a trigger signal is formed which instructs the data acquisition system to read out all the channels that have non-zero information. It is more efficient to use the calorimeter-tagger coincidence as a primary physics trigger since using the tagger signal alone would flood the data acquisition due to the high rate of tagging counter signals, most of which represent photons which just passed through the target without producing an event of interest. Figure 7 illustrates the basic ideology behind the primary trigger setup for the *PrimEx* experiment.

The *PrimEx* data acquisition system used multi-hit time to digital converters (LeCroy LRS1877) with a maximum range of 32 μs, double pulse resolution of ~ 20 ns, and with the capability of storing up to 16 hits per trigger event per channel in a LIFO (Last In First Out) mode. The range of the TDC and the LIFO limit are programmable and for the *PrimEx* experiment were set to 16 μs and 10 hits, respectively. The capabilities of these TDCs allows for significant improvement on the analysis techniques of tagged photon experiments described in Ref. [10].

Since only a timing coincidence is required between the calorimeter and tagger MOR (OR of eleven T-counters) signals to form a trigger, there are two scenarios for losing prompt π^0 - tagger coincidence yield due to the TDC dead-time (double pulse resolution) and LIFO limit:

1. An entire event is lost due to TDC dead-time, *i.e.,* there was no signal from tagging counters to form a prompt coincidence with the calorimeter signal but the data acquisition system is ready to take data. From the stand point of photon flux determination, this case is very similar to the

situation where the data acquisition system is busy reading out data and is not accepting any triggers.

2. A photon producing a π^0 may be lost due to the LIFO limit but the triggering condition might be satisfied by a signal from another tagging counter. Just like in the previous case such events will not contribute to the tagged yield.

To measure a cross section, one is interested in the number of tagged photons on the target which have the potential to produce a prompt coincidence between the tagger and the photo-induced event of interest, which in this case is a π^0 in the HYCAL calorimeter. While the yield of π^0 - tagger prompt coincidences is reduced by the TDC intrinsic dead-time, LIFO limit and the DAQ readout dead-time, below (in sections 6.1 and 6.2) we describe a method for determining the photon flux which is affected in the same manner as the π^0 - tagger prompt coincidence yield. This obviates the need to correct for the number of the tagged photons lost due to these effects.

The rate of tagged photons can be determined from the timing information, recorded by tagging counters, via sampling of the number of hits for a small fraction of the time. An assumption is then made that these samples are representative of the detectors' rates for the times when no data are recorded. This can be used to extrapolate to all times in order to determine the total number of tagged photons represented by a given data sample. Since one is interested in the number of tagged photons that have the potential to produce a prompt π^0 - tagger coincidence, the timing information from only fully reconstructed hits in the tagger needs to be considered. A fully reconstructed hit requires a hardware timing coincidence between the PMTs fitted to each of the ends of a T-counter that is simultaneously in time with a hit in an E-counter. The coincidences between "E-" and "T-" counters are also subject to a geometric matching where the two counters are required to be on an electron trajectory which is consistent with the magnetic optics of the tagger.

The LeCroy 1877 TDCs with which the T-counters were equipped operated in common stop mode during the *PrimEx* experiment. A T-counter signal passed through a constant fraction discriminator and was split into two signals. One signal started the TDC and the other signal passed through an E-T coincidence/MOR module. Assuming a coincidence between the left and right T-counter PMTs, the MOR module sent a signal to the trigger supervisor when any E-T coincidence was obtained. If a signal from the calorimeter was in coincidence with the MOR signal, the trigger supervisor issued a common stop trigger signal to all electronics involved in the data acquisition. Figure 8 shows an example of a timing spectrum of hits reconstructed for a single T-counter in the tagger. Note that the abscissa in Fig. 8 (*top*) is presented on a log scale. The peak in the timing spectrum at around 100 ns corresponds to the time difference between the two split signals from a single T-counter, *i.e.,* is associated with the events when this particular T-counter was involved in the trigger. The flat accidental background comes from signals that were not involved in the trigger but were accidental hits recorded due to the common stop/multihit nature of T-counter TDCs.

One obvious effect seen in Figure 8 (*bottom*) is that the number of hits trails off on the right side of the spectrum due to the LIFO limit. Since during the *PrimEx* experiment the LeCroy 1877's were used in a common stop mode, earlier times are to the right and later times are to the left in this plot. The LeCroy 1877 TDC will always report the latest hits. Thus when the LIFO buffer fills up, the earlier hits are overwritten by later ones.

6.1. The "out of time" method

The tagged photon flux at the target can be determined by means of sampling the "out-of-time" (OOT) electron hits in the tagger T-counters. The term "out-of-time" electron refers to any fully reconstructed electron which was not involved in the formation of the trigger signal. The idea is to simply count the number of hits in a particular T-counter within some user defined time window w and divide by the size of the time window. Since even high rate detectors on average tend to have only a few hits per event, it is necessary to integrate over many events to obtain an accurate value for the rate.

When counting hits, it is important to discard those that could be associated with the trigger. Hits which are correlated with the trigger are biased and will artificially increase the calculated rate. The OOT window, w, should be defined in such a manner that it does not include the trigger coincidence peak region but can include areas both before and after the trigger peak. One drawback of this rate sampling technique is that it is potentially vulnerable to beam intensity variations since it will tend to sample more often when the beam intensity is higher. As such, the "clock trigger" method was implemented as described below.

6.2. The "clock trigger" method

To ensure that the calculated rates are not biased by beam intensity variations, a 195 kHz clock trigger, which was completely uncorrelated with the electron beam current, was implemented in addition to the physics trigger. The clock triggers were pre-scaled so that the data are dominated by events of physics type that are of interest. The pre-scale factor depends on the electron beam intensity and on the type of the data taking run, *i.e.,* pion photoproduction, or calibration runs involving Compton scattering or pair production. Figure 9 shows a sample timing distribution for hits reconstructed in a single T-counter recorded with the clock trigger. As in the case of the tagger MOR-calorimeter coincidence trigger, one can see a depletion of hits due to the LIFO limit starting at around 10μs, but the peak characteristic of a beam related trigger is missing.

The same out of time window, w, shown in Figure 9, is used when calculating the rates with either clock or physics triggers. It was chosen to be 7μs for all T-counters spanning from 500 to 7500 ns, thus avoiding the coincidence peak in the case of MOR-calorimeter coincidence trigger and the region affected by the LIFO limit for both triggers. Extra effort has been put into checking that the distribution of hits inside the out of time window is flat.

Following the above described procedure for an electron rate calculation we have:

$$r^i = \frac{n_e^i}{w \cdot n_{trigger}} \quad (6)$$

where r^i is the rate of T-counter i, n_e^i is the number of hits within the out of time window of width w and $n_{trigger}$ is the number of times the T-counter i could have had a hit, *i.e.,* the number of triggers. Equation 6 assumes Poisson statistics for "out of time" electrons and it assumes constant electron rate per T-counter.

The *PrimEx* experiment utilized a second generation of the JLab designed Trigger Supervisor (TS) module. This module is designed specifically to optimize event rates for Fastbus and VME based data acquisition systems like those commonly used in intermediate and high energy physics experiments. One new feature in the second generation model is the inclusion of two scalers dedicated to measure the live-time of the DAQ. Both scalers are driven by a 195.3160 ± 0.0045 kHz internal clock. One of these scalers is live-time gated while the other is free-running. The ratio of the two gives the fractional live-time of the data acquisition system.

To determine the tagged photon flux, one needs to know the number of the hits in a detector during the live-time of the data sample. This can be obtained using only the live-time gated scaler to calculate the actual live-time as shown below. Note that the free running scaler is not needed since both the π^0 yield and the photon flux are affected by the data acquisition system dead time in the same way:

$$T_{live} = n_{gated} \cdot \beta \quad (7)$$

where n_{gated} is the number of scaler counts from the gated TS scaler and $\beta = \frac{1}{clock\ frequency}$, *i.e.,* $\beta = 5119.9083 \pm 0.0002$ ns.

The *PrimEx* data acquisition system had the option of a variety of triggers which could be prescaled as needed. In this case, it was a prescaled 195 kHz clock. When this clock was responsible for the event trigger, a bit was set indicating it was a clock trigger. The number of such triggers could thereby be tallied in the off line analysis. Given Equation 7, the total number of electrons counted by T-counter i during the time the data acquisition was live is expressed by:

$$N_e^i = r^i \cdot T_{live} = \frac{n_e^i}{w \cdot n_{trigger}} \cdot n_{gated} \cdot \beta \tag{8}$$

The number of tagged photons N_γ^i in T-channel i which can reach the physics target can be calculated as:

$$N_\gamma^i = N_e^i \cdot R^i_{absolute} \tag{9}$$

where N_e^i is the number of counts per T-channel i and $R^i_{absolute}$ is the tagging ratio, which is determined in the TAC analysis.

The value of the window width w was obtained using the TDC conversion factor specified by the manufacturer. As the total rms error is 400 psec, the integral non-linearity is less the 25 ppm full scale, the full scale error is $\pm$ 0.0025%, and the long term stability is less than 100 ppm/year[11], the uncertainty in w is negligible.

7. Relative photon flux normalization with pair production

The pair spectrometer is designed for relative in-situ monitoring of the photon flux and is an essential part of the *PrimEx* experimental set up. It uses the physics target to convert a fraction of the photons into e^+e^- pairs which are deflected in the field of a dipole magnet downstream of the target and are registered in plastic scintillator detectors on both sides of the beam line. The relative tagging ratio for a given T-counter is given by Eq. 5.

During the *PrimEx* production data taking, electron-positron pairs in coincidence with the clock trigger were measured to determine $R^i_{relative}$. As with the physics triggers of interest, the clock trigger also enabled a direct count of the number of electrons detected by the tagging counters for the determination of $R^i_{relative}$, with the advantage of being insensitive to beam intensity variations.

7.1. PS-tagger coincidence window and background

The events reconstructed in both the tagger and the pair spectrometer are randomly distributed in time with respect to the clock trigger. The spectrum of tagger - pair spectrometer time differences exhibits a prompt coincidence peak and a random background. A sample timing spectrum is shown in Fig. 10.

In general, taking the difference of two random distributions, defined over the same interval, results in a triangular shape distribution. This provides an exact background model, which enables one to easily simulate the "background only" part of the spectrum.

7.2. Effect of incident electron beam intensity on relative tagging ratios

In order to justify the use of the absolute normalization of the photon flux obtained at the low electron beam currents of the TAC runs for the calculation of the number of tagged photons on target, it is important to demonstrate the independence of the $R^i_{relative}$ on the electron beam current. The relative tagging ratios, defined by Eq. 5, provide valuable confirmation of this procedure as they can be measured at the low currents of the TAC runs as well as at high electron beam currents of the production data taking runs.

R^i_{rel} was measured for electron beam currents ranging from 0.08 to 100 nA. The results for a representative T-counter are shown in Figure 11, where the percent deviation from the mean value for this T counter is indicated for each individual intensity. For these measurements of the rate dependence of the relative tagging ratios, a tagger Master-OR trigger was used. Figure 12 shows the percent deviation from the mean of the measured R_{rel} as a function of beam current integrated over the full photon tagging energy range (*i.e.*, treating tagging counters T1-T11 as one single counter) where it can be seen that the variation is at the $\pm 1\%$ level.

7.3. Stability of relative tagging ratios

The relative tagging ratios have to be not only intensity independent but also stable from run to run, *i.e.,* in time, to within 1%. The time stability of the relative tagging ratios measured by the pair spectrometer justifies the use of a single set of absolute tagging ratios measured by the TAC for the tagged photon flux calculation. As such, to achieve a 1% level tagged photon flux measurement integrated over the tagged photon energy range, any deviation from the nominal value of the $R_{relative}$ has to be carefully investigated and if possible corrected. In the discussion that follows, the data from eleven T-counters were combined together and the part of the focal plane of the tagger that is of interest to the *PrimEx* experiment is treated as one single counter, thus enabling a reduction in the statistical error.

Fig. 13 shows the time dependence of $R^{combined}_{relative}$ - the combined relative tagging ratio for data taken with a carbon target. The two black solid lines on the graph represent a $\pm1\%$ deviation from the weighted average for run numbers less than 4800. One can see that for the last group of runs (run number > 5150), the relative tagging ratio falls off. This deviation, which was found to be associated with high current beam delivery to experimental Halls A and C at Jefferson Laboratory, is larger than 1% and indicates that a correction is needed when calculating the photon flux for this group of runs.

The change in $R^{combined}_{relative}$ in Fig. 13 can arise from the tagger registering extra electrons which do not produce photons, or a part of the photon beam being lost before reaching the physics target (or TAC, since the same effect has been seen in absolute tagging ratios), or both. In either case, the measurement of the relative tagging ratios enables a correction to be made to compensate for these changes in experimental conditions on a run-by-run basis.

The pair spectrometer also provides information on the performance of the photon tagger. Fig. 14 shows a $\sim 3.5\%$ drop in the fraction of the photons on the target which are tagged by tagging counters T1 through T11, $\frac{N^{PS}_{e^+e^-\cdot e^i}}{N^{PS}_{e^+e^-}}$, when going from the 80 nA (runs 4747 - 4768) to the 130 nAmp (runs 5158-5210) groups of runs. This overall drop can be explained by a drop in the absolute efficiency (hardware and reconstruction) of the tagging counters with an increase of the beam current.

In Fig. 15 is plotted the ratio of the number of e^+e^- pairs registered in the pair spectrometer to the number of electrons registered in the tagger. The plot shows a $\sim 3.2\%$ rise when going from the 80 nA group of runs to the 130 nA group, which again can be explained by inefficiency of the tagger at high beam intensities.

A strength of the photon tagging technique is, of course, the fact that the absolute efficiencies of the photon tagging detectors need not be known in the photon flux determination. Such investigations of efficiencies, however, can be of relevance in determining the optimal beam current at which to run a given experiment.

8. Conclusions

Using the techniques described here, the Jefferson Laboratory *PrimEx* Collaboration has performed a high precision measurement of the neutral pion lifetime whereby an accuracy at the 1% level in the tagged photon flux integrated over the tagging energy range was achieved. Major elements include the implementation of multi-hit time to digital converters, electron counting techniques involving sampling of the post bremsstrahlung electron rates, and the implementation of a pair spectrometer for continuous, on-line measurement of relative tagging ratios. While this discussion has been in the context of a measurement of the photoproduction of neutral pions, many of these techniques are applicable to other high precision photon tagging experiments.

References

[1] P. Argan, *et al.*, Nucl. Instr. and Meth. A228 (1984) 20.

[2] J.D. Kellie, *et al.*, Nucl. Instr. and Meth. A241 (1985) 153.

[3] T. Terasaw, *et al.*,Nucl. Instr. and Meth. A248 (1986) 429.

[4] C.E. Thorn, *et al.*, Nucl. Instr. and Meth. A285 (1989) 447.

[5] I. Anthony, *et al.*,Nucl. Instr. and Meth. A301 (1991) 230.

[6] N. Bianchi, *et al.*, Nucl. Instr. and Meth. A317 (1992) 434.

[7] Detemple, *et al.*, Nucl. Instr. and Meth. A321 (1992) 479.

[8] S. J. Hall, *et al.*, Nucl. Instr. and Meth. A368 (1996) 698.

[9] D. Sober, *et al.*, Nucl. Instr. and Meth. A440 (2000) 263.

[10] R.O. Owens, Nucl. Instr. and Meth. A288 (1990) 574.

[11] http://teledynelecroy.com/lrs/dsheets/1877.htm.

[12] M. Kubantsev, *et al.*, AIP Conf. Proc. 867 (2006) 51.

[13] I. Larin, *et al.*, Phys. Rev. Lett. 106:162303, 2011.

[14] H.A. Bethe and L.C. Maximon, Phys. Rev., vol. 93, no. 4, (1954) 768.

[15] F. Gougnaud, *et al.*, International Conference on Accelerator and Large Experimental Physics Control Systems, Triest, Italy, (1999) 45.

[16] G. Bellettini *et al.*, Il Nuovo Cimento, vol. 66, no. 1, (1970) 243.

[17] V.I. Kryshkin *et al.*, Sov. Phys. JETP, vol. 30, no. 6, (1970) 1037.

[18] G. Bellettini *et al.*, Il Nuovo Cimento, vol. 40, no. 4, (1965) 1139.

[19] A. Browman *et al.*, Phys. Rev. Lett., vol. 32, (1974) 1067.

[20] A. Browman *et al.*, Phys. Rev. Letts., vol. 33, no. 23, (1974) 1400.

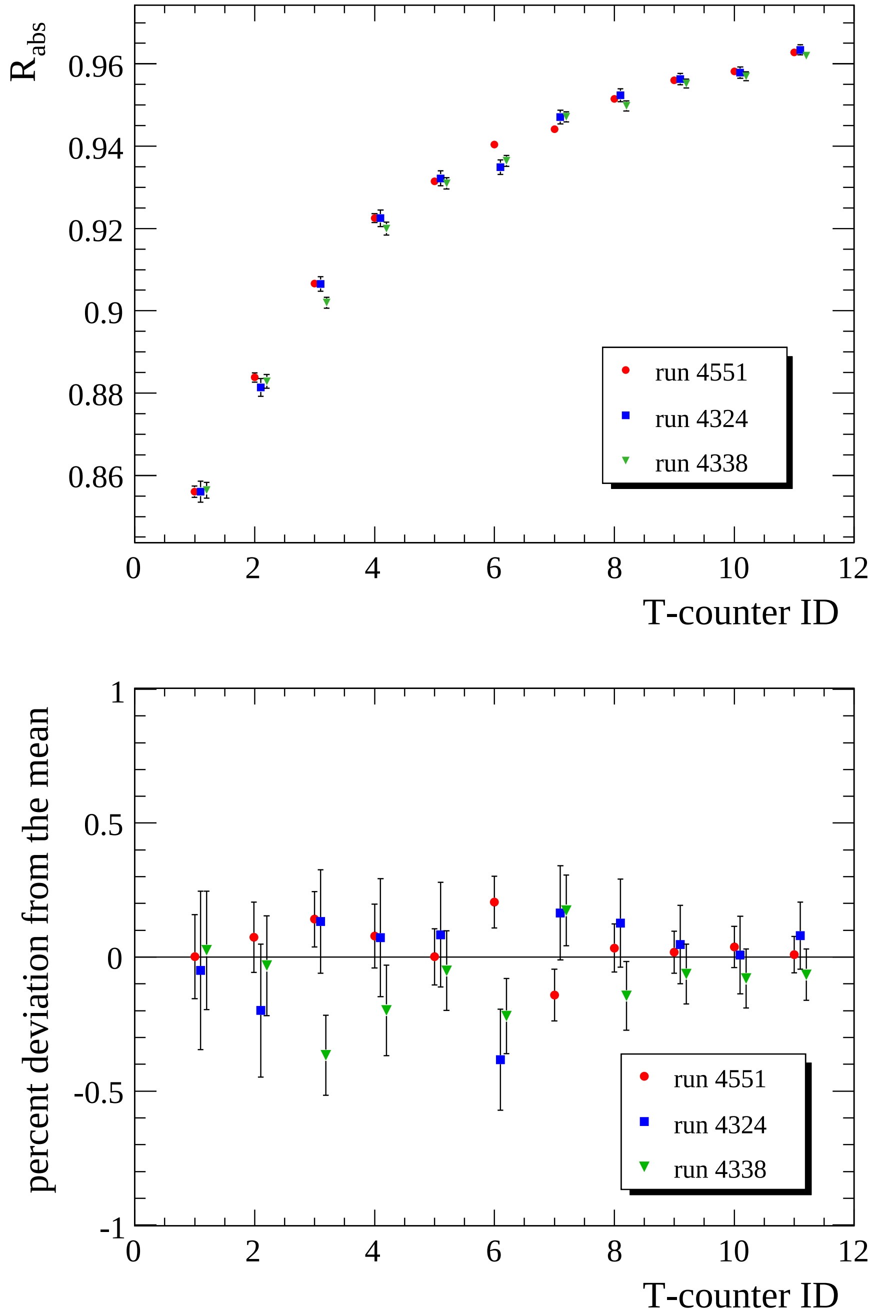

Figure 4: (top) R_{abs} measured for three runs which were separated in time during the data taking. The points for the three runs are displaced horizontally for clarity. (bottom) Percent deviation from the mean. The photon energy range is from 4.9 GeV (T counter 11) to 5.5 GeV (T counter 1). The 12.7 mm diameter photon collimator was removed for these measurements.

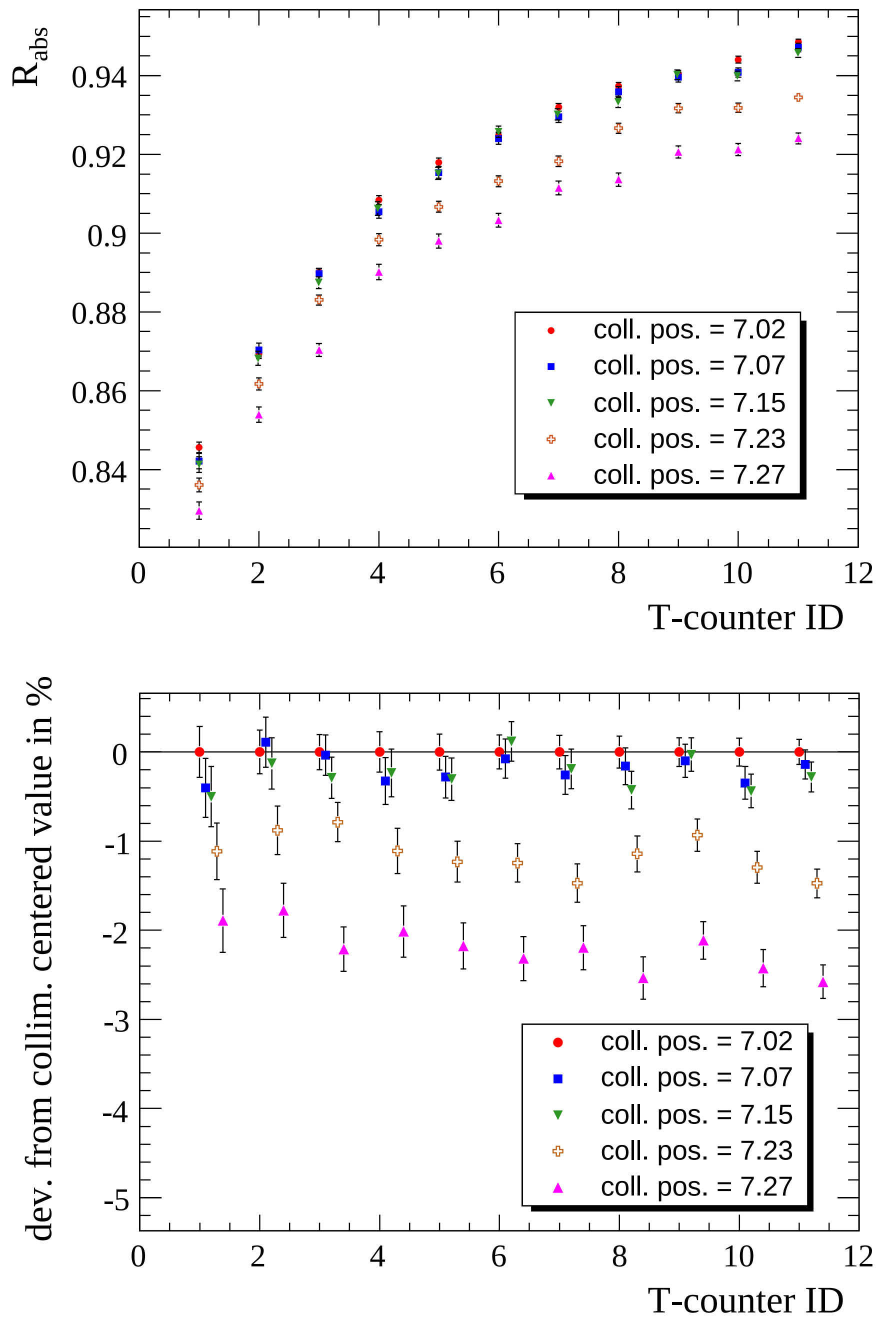

Figure 5: (top) $R_{absolute}$ measured for five different collimator positions measured in inches. (bottom) Percent deviation from the measurement taken with collimator in its nominal position ($7.02in$). The photon energy range is from 4.9 GeV (T counter 11) to 5.5 GeV (T counter 1). The points for the three runs are displaced horizontally for clarity.

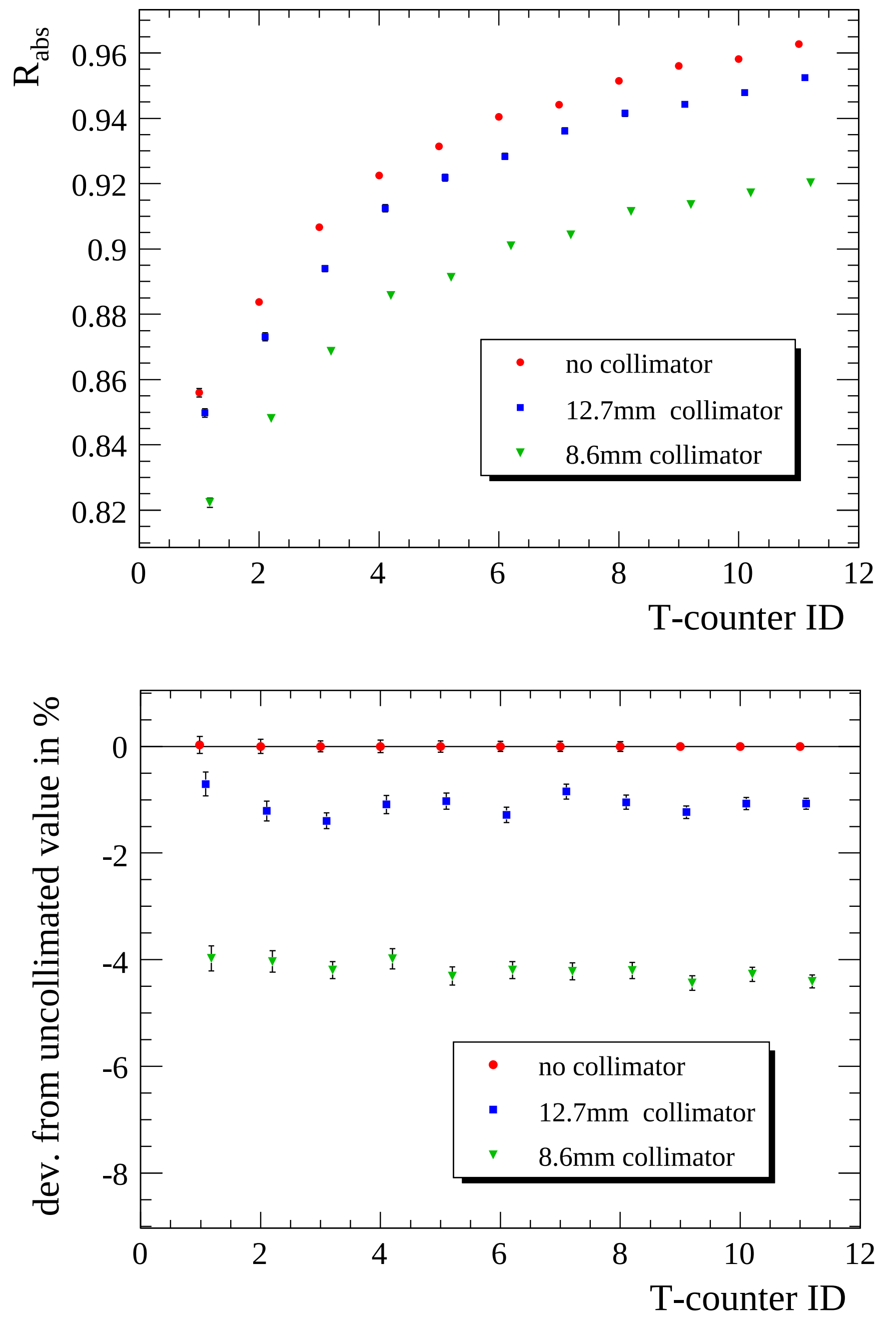

Figure 6: (top) $R_{absolute}$ measured for three different collimator sizes. (bottom) Percent deviation from the uncollimated value. The photon energy range is from 4.9 GeV (T counter 11) to 5.5 GeV (T counter 1).

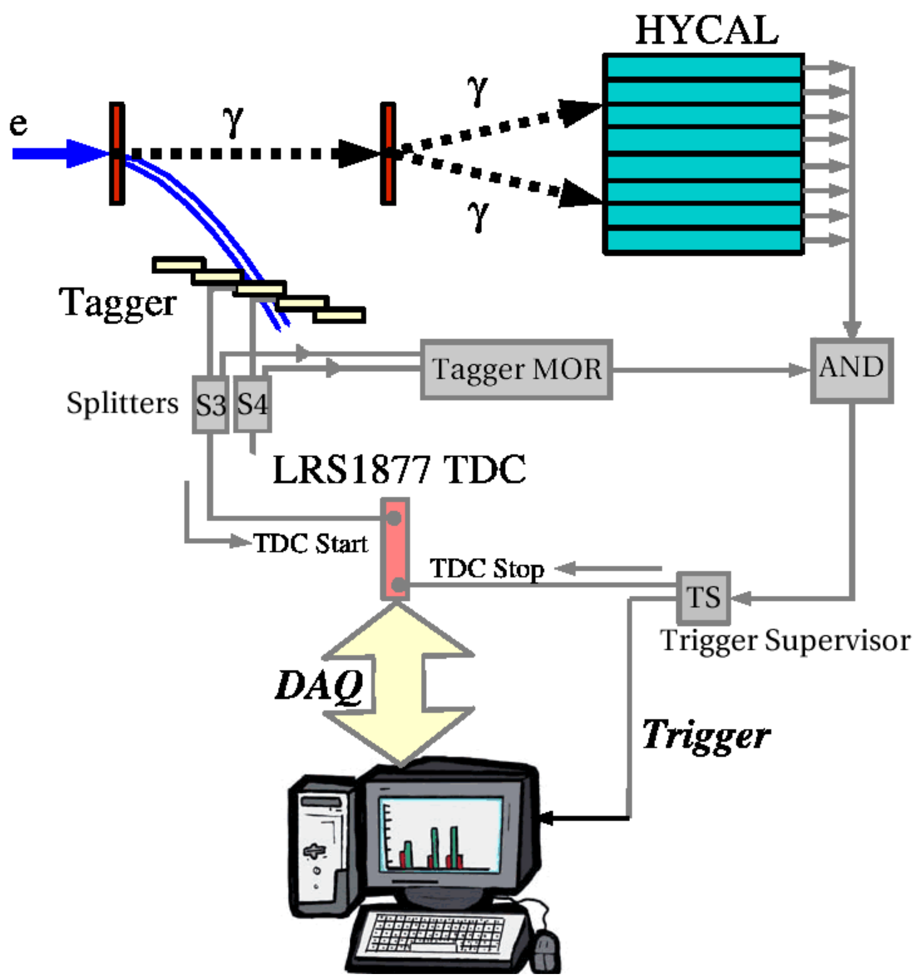

Figure 7: A schematic of the trigger setup.

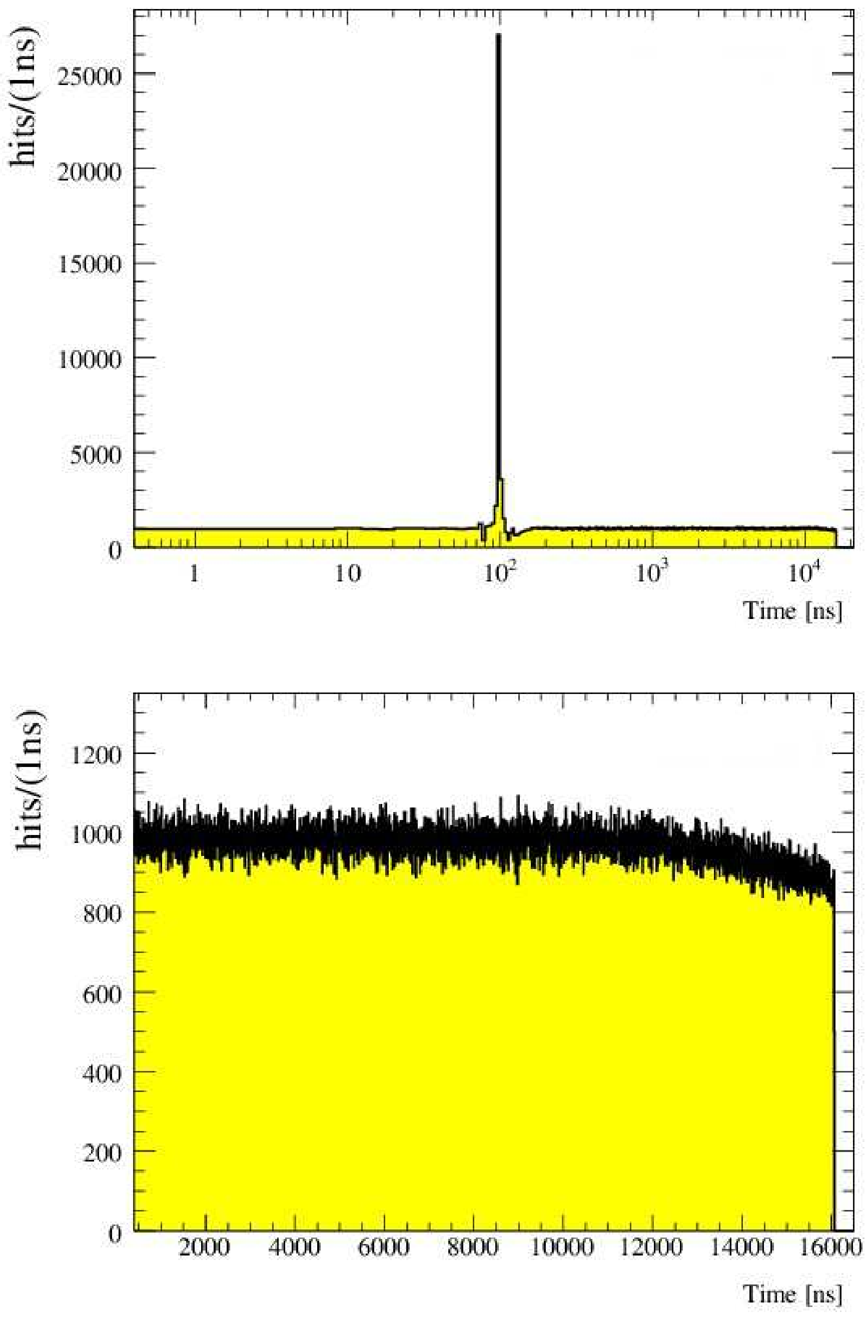

Figure 8: (top) Time spectrum of hits reconstructed for a single T-counter. (bottom) A close up of the top plot illustrating the drop off of the number of hits due to LIFO limit.

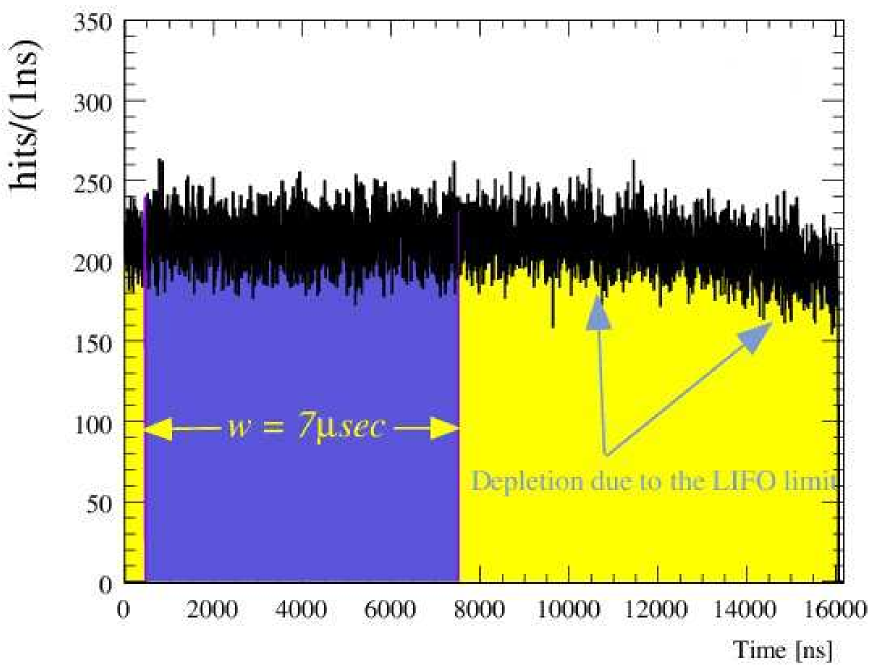

Figure 9: Timing spectrum of hits reconstructed for a single T-counter. These data were taken with clock triggers.

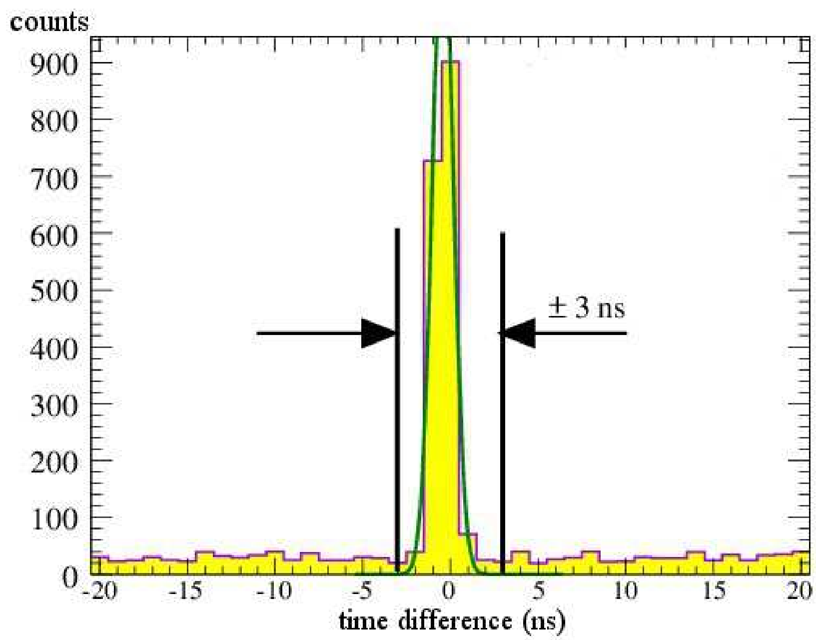

Figure 10: Distribution of time differences for events reconstructed in the tagger and pair spectrometer showing the ±3.0 ns timing coincidence window.

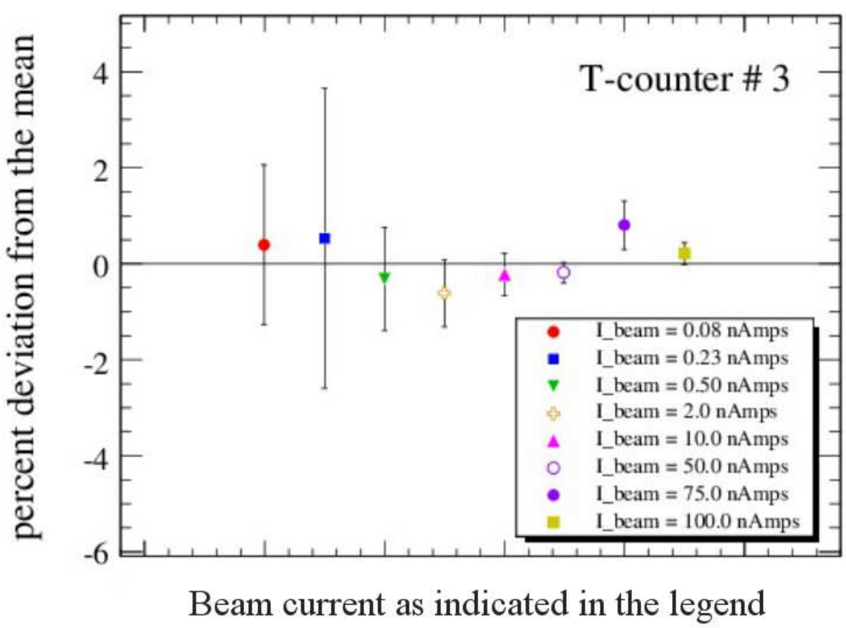

Figure 11: Percent deviation from the mean for relative tagging ratio measurements, R^i_{rel}, for T-counter #3 for electron beam currents ranging from 0.08 to 100 nA.

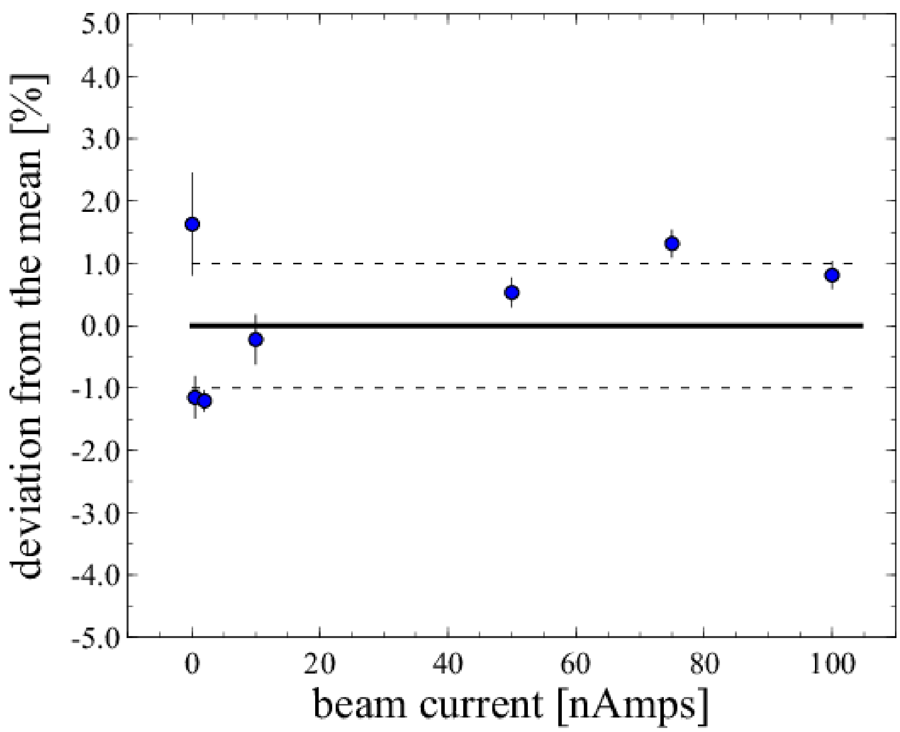

Figure 12: Percent deviation from the mean for relative tagging ratio measurements, R_{rel}, integrated over the photon tagging energy range (*i.e.*, treating the tagger as one single counter) for electron beam currents ranging from 0.08 to 100 nA. The dashed lines indicate a $\pm 1\%$ deviation from the mean.

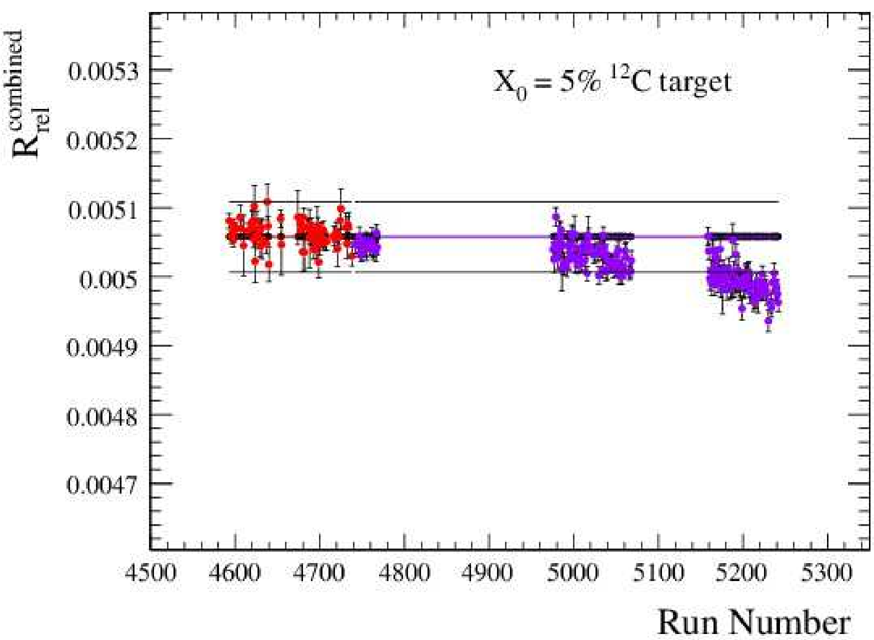

Figure 13: Run-to-run stability of $R_{rel}^{combined}$ - relative tagging ratio combined for eleven T-counters – carbon target.

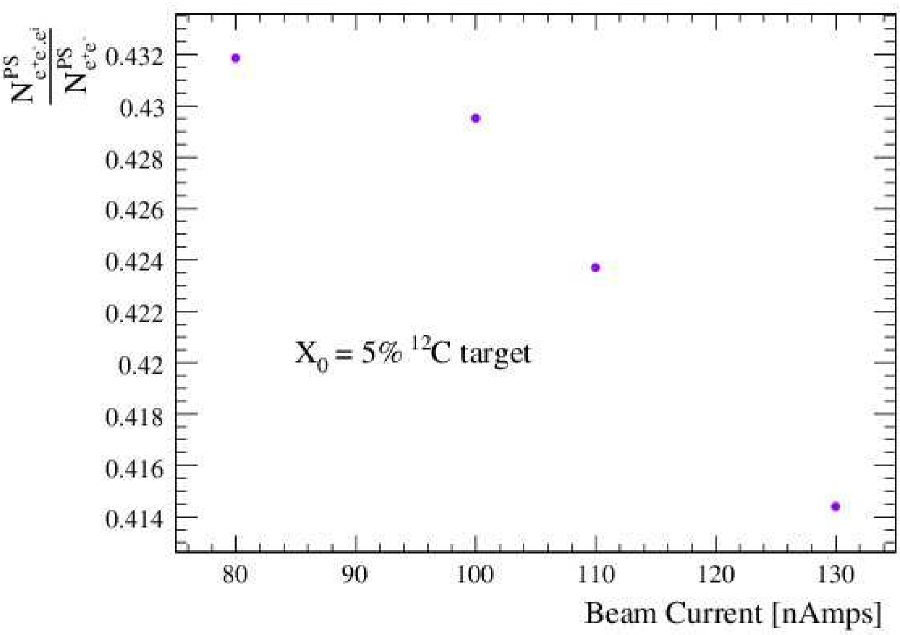

Figure 14: $N^{PS}_{e^+e^-e^i}/N^{PS}_{e^+e^-}$ vs. beam current, combined for eleven T-counters and averaged for all runs with the same current, reflecting the loss of absolute efficiency of the tagger.

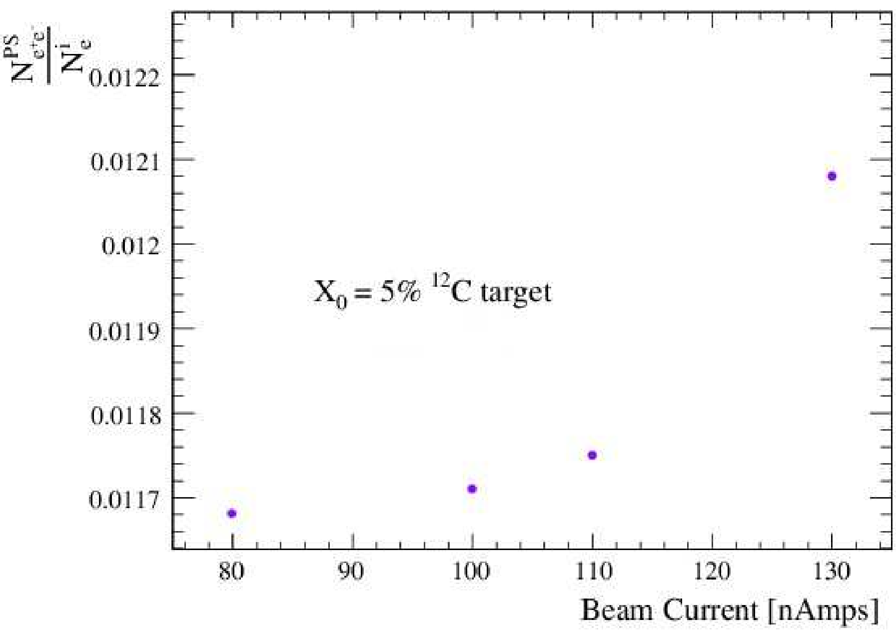

Figure 15: $N^{PS}_{e^+e^-}/N^i_{e^-}$ vs. beam current, combined for eleven T-counters and averaged for all runs with same current, reflecting the loss of absolute efficiency of the tagger.